Optics Letters

Efficient generation of quantum light using bound states in the continuum in silicon-nanowire slow-light waveguides

Runzhi Cao,[1,2] Tianjiao Sun,[1,2] Chong Sheng,[1,2,*] Tianyu Zhang,[1,2] Jiaxuan Zhou,[1,2] Shining Zhu,[1,2] and Hui Liu[1,2,3]

[1]National Laboratory of Solid State Microstructures, School of Physics, Collaborative Innovation Center of Advanced Microstructures, Nanjing University, Nanjing, Jiangsu 210093, China
[2]Collaborative Innovation Center of Advanced Microstructures, Nanjing University, Nanjing, Jiangsu 210093, China
[3]liuhui@nju.edu.cn
*csheng@nju.edu.cn

Received 4 November 2025; revised 14 January 2026; accepted 25 January 2026; posted 26 January 2026; published 11 February 2026

On-chip quantum light sources are a fundamental component of integrated photonic quantum information systems. However, their performance is fundamentally limited by weak nonlinear interactions and high propagation losses, which hinder efficient generation. Here, we propose a fishbone-modulated grating structure on a silicon-nanowire waveguide to significantly enhance spontaneous four-wave mixing. The proposed structure achieves a quantum-light generation efficiency two orders of magnitude higher than conventional silicon-nanowire waveguides. Specifically, we exploit a Su–Schrieffer–Heeger-like topological interface to slow light in the waveguide, thereby enhancing the nonlinear coefficient. Moreover, we leverage the principles of bound states in the continuum to optimize the modulated gratings on the waveguide, achieving ultra-low waveguide propagation loss. The simultaneous realization of the slow-wave effect and ultralow loss effectively enhances the spontaneous four-wave mixing process in silicon. Our approach opens new possibilities for designing enhanced nonlinear nanophotonic devices using various nonlinear optical materials.

https://doi.org/10.1364/OL.583797

Introduction. Quantum light sources play a critical role in quantum information processing applications, including quantum key distribution, quantum teleportation, and quantum computing. Recent advancements in integrated photonic quantum technologies [1,2] have driven the growing demand for compact and scalable quantum light sources. To meet this requirement, nonlinear crystals have been structured into thin-film configurations on insulating substrates, thereby enhancing quantum-light generation efficiency. Representative platforms [3–9] such as silicon-on-insulator (SOI), lithium niobate-on-insulator (LNOI), and gallium nitride-on-sapphire (GNOI) exemplify this approach, enabling scalable implementations of integrated quantum photonic systems. Among these, SOI-based quantum-light generation has emerged as a leading candidate for scalable quantum information processing [10], owing to its compatibility with complementary metal-oxide-semiconductor (CMOS) fabrication processes. By leveraging spontaneous four-wave mixing (SFWM) in silicon, various on-chip quantum source architectures have been developed, including nanowire waveguides [11], microring resonators [12], coupled microring systems [13], two-dimensional (2D) photonic crystal defect waveguides [14,15], and topologically protected ring resonator arrays [16,17]. However, practical implementations of these schemes encounter inherent limitations. For example, nanowire waveguides necessitate prohibitively long propagation lengths due to their limited nonlinearity coefficients, restricting further miniaturization. Microring waveguides require stringent fabrication tolerances. Although coupled microring resonators and 2D photonic crystal defect waveguides exploit large nonlinearity coefficients induced by the slow-wave effect [13–15,18,19], their high propagation losses [20] inevitably lead to compromised quantum-light generation efficiency.

Recently, bound states in the continuum [21–23] (BICs) have emerged as a promising paradigm for designing integrated photonic devices with novel functionalities. Specifically, their capability to suppress radiative losses enhances light confinement in waveguides, enabling on-chip artificial structures to simultaneously achieve low propagation losses and slow light functionality. Examples include ultra-low-loss on-chip zero-index photonic crystals and meta-waveguides [24–27], as well as BICs-based photonic integrated circuits [28–30]. Notably, a recent study demonstrated ultra-low-loss electro-optic modulators [31] using apodized-grating nanowire slow light waveguides [32–34], where BICs significantly mitigate scattering losses arising from grating corrugations. However, few studies have harnessed this unique advantage of BICs in slow light waveguides to realize on-chip bright quantum-light sources.

In this work, we propose a scheme for achieving high-efficiency quantum-light generation using a fishbone-modulated silicon-nanowire waveguide with the aid of BICs and the slow

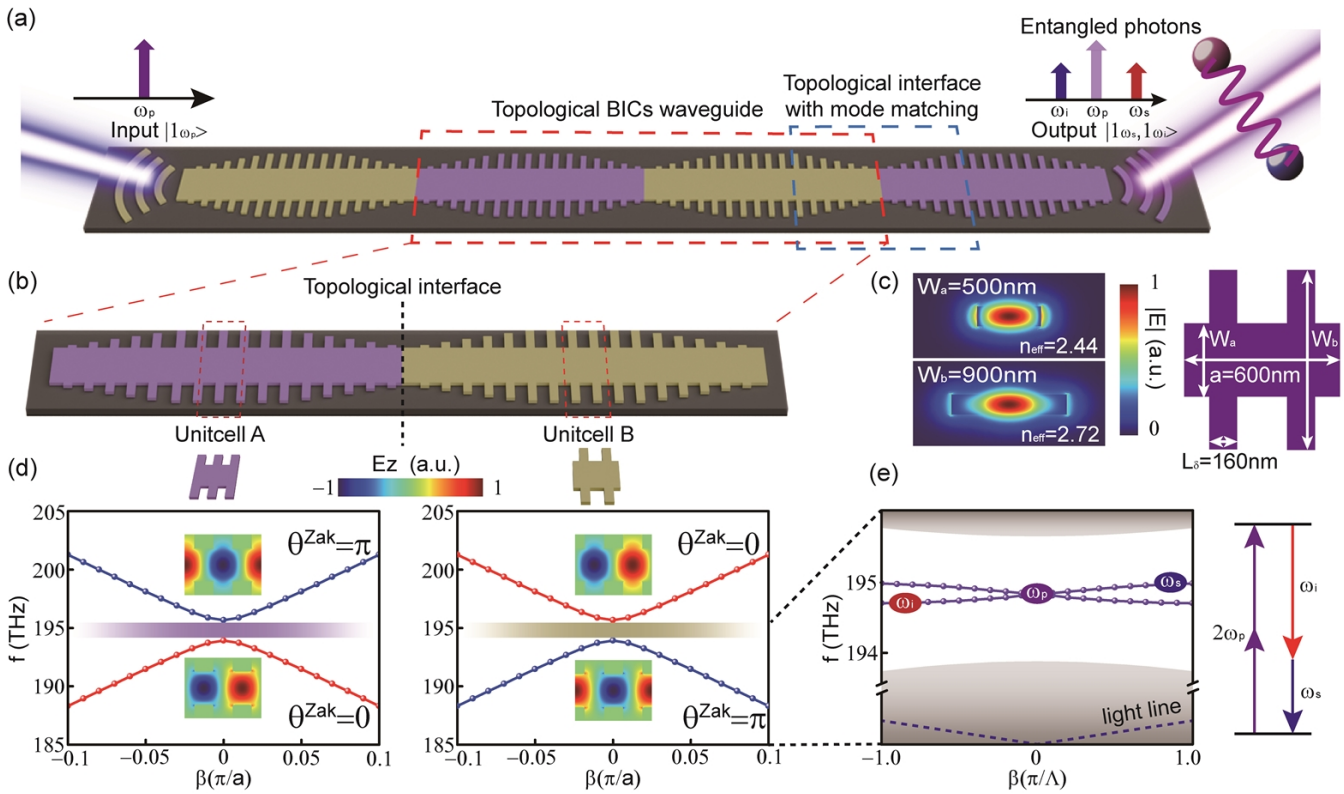

Fig. 1. (a) Efficient generation of photon pairs using a modulated superlattice nanowire waveguide with the aid of BICs and the slow light effect. The different false colors indicate photonic lattices composed by different unit cells. (b) Schematic of superlattice composed by 75 unit A cells and 75 unit B cells, whose length is 90 μm. (c) Mode distribution of gratings with different widths. (d) The dispersion and Zak phase of two types of 1D photonic crystal waveguides comprising of unit cell A or B, the inserts illustrate the eigenmode of different bands at Γ point. (e) Dispersion of the 1D superlattice photonic crystal waveguide with topological interface state.

light effect. This modulated waveguide exhibits an ultralow loss of 0.25 dB/mm and a large group refractive index (~20), leading to a two-order-of-magnitude enhancement in generation efficiency during the SFWM process compared with conventional silicon-nanowire waveguides. Our design establishes a paradigm for the development of compact, scalable, and highly efficient on-chip quantum-light sources.

Working Principle and Device Design. To achieve high generation efficiency of correlated photon pairs through SFWM based on a single silicon-nanowire waveguide, we first start with the generation of the photon-pair flux f (the number of photons generated per unit frequency and per unit time) at a small pump power P as the frequency ω over a propagation distance L, is given by [12]:

$$f \cong \left(\frac{\omega n_2}{cA_{eff}} PL\, exp\,(-\alpha L)\right)^2 \mathrm{sinc}^2\left(\frac{\beta_2 \Omega^2 L}{2}\right), \qquad (1)$$

where β_2 is the group velocity dispersion of waveguide, α is the loss coefficient, c is the speed of light, n_2 is the intrinsic nonlinearity, Ω is the frequency detuning, A_{eff} is the effective mode area of this waveguide that can depicted as [35]:

$$A_{eff} = \frac{3}{n_g^2 n_c^2} \frac{\left(\int_S n_w^2 |F|^2 ds\right)^2}{\int_c F^* \cdot \left[2|F|^2 F + (F \cdot F)\, F^*\right] ds}, \qquad (2)$$

where F is the normalized mode distribution of the waveguide mode, n_c is the effective refractive index of the waveguide, and n_g is the group refractive index of the waveguide. By analyzing Eqs. (1) and (2), we identify that enhancing the generation efficiency of correlated photon pairs can be achieved by minimizing waveguide loss and improving the group refractive index. To address this, we propose a fishbone-modulated superlattice nanowire silicon waveguide with the aid of BICs and the slow light effect, as illustrated in Fig. 1(a), whose design parameters are given in Supplement 1. Specifically, this structure, incorporating a Su–Schrieffer–Heeger (SSH)-like topological interface state, effectively enhances the group refractive index. Simultaneously, we leverage the principles of BICs to achieve ultra-low waveguide loss.

To realize a high group refractive index, we employ two distinct grating units, A and B, to form a fishbone-modulated superlattice waveguide. These grating units exhibit two different geometric symmetries, with the symmetry center of unit A (B) located at the center of the wide (narrow) part of the grating. As demonstrated in Fig. 1(c), the modulation of the nanowire width results in variations in the effective mode index. By periodically modulating the nanowire width using gratings, we create a one-dimensional photonic crystal waveguide analogous to a classic Su–Schrieffer–Heeger (SSH) model. Using full-wave simulations (COMSOL Multiphysics), we calculate the dispersion characteristics of this 1D photonic crystal waveguide composed solely of unit A or unit B. As shown in Fig. 1(d), these two types of 1D photonic crystal waveguides exhibit identical dispersion characteristics but different Zak phases for the same band. When combining these two types of 1D photonic crystal waveg-

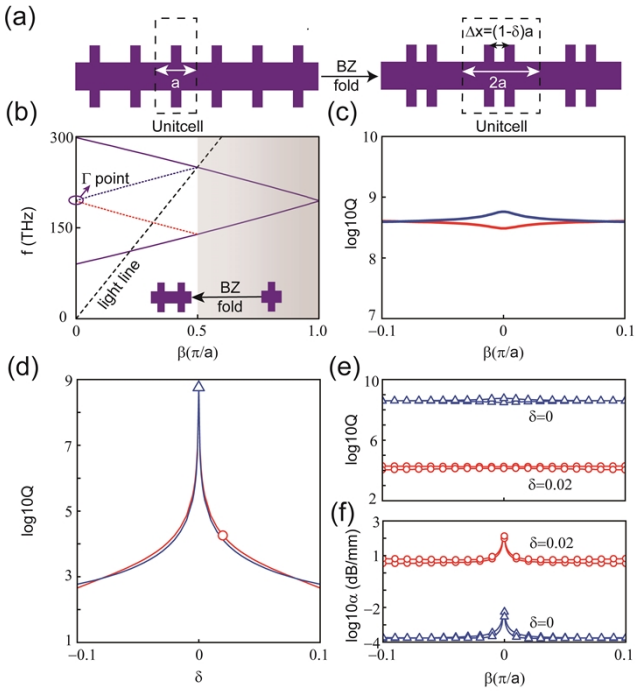

Fig. 2. (a) BZ folding of photonic lattices. (b), (c) Dispersion and Q factor of BZ-folded photonic lattices. (d) Q factor of the unit cell with different δ. (e), (f) Q factor and loss of BICs ($\delta = 0$) and non-BICs ($\delta = 0.02$) lattices.

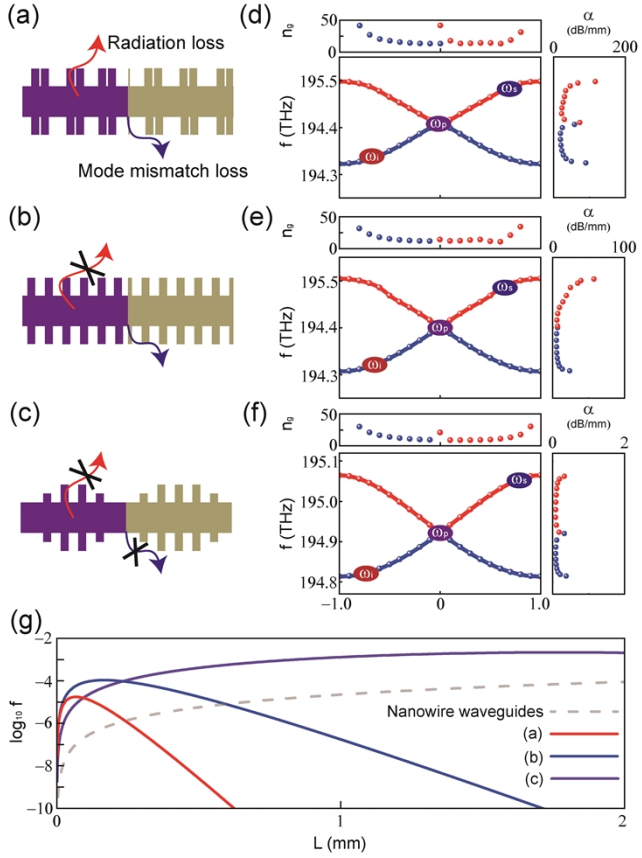

Fig. 3. (a) Superlattice without BICs or mode matching. (b) Superlattice with BICs but without mode matching to inhibit the radiation losses. (c) Superlattice with BICs and mode matching to inhibit the two types of losses. (d)–(f) Dispersion of different types of superlattice respectively for case (a)–(c), the side illustration is the group refractive index and loss. (g) Flux of different types of superlattice respectively for case (a)–(c), where the gray dashed line represents a conventional nanowire waveguide.

uides to form a superlattice, as shown in Fig. 1(b), a topological interface state emerges, enabling a reduction in light velocity, as illustrated in Fig. 1(e). Consequently, the group refractive index of the pump, signal, and idler waves is significantly enhanced, reaching approximately (n_g ~20), which is nearly five times higher than that of a conventional straight nanowire silicon waveguide. This enhanced group refractive index improves the nonlinear coefficient, as it is positively correlated with n_g.

Generally, introducing extra protrusions to a straight waveguide inevitably induces radiation loss. However, a prominent type of BICs can mitigate this loss through destructive interference, as it shares a common decay channel for two radiative modes. Inspired by this mechanism, we leverage the principles of BICs to optimize the modulated grating on an SSH-like 1D photonic crystal waveguide, thereby reducing radiation loss. Specifically, we employ the Brillouin zone (BZ)-folding method to realize this BICs-assisted waveguide. Initially, we calculate the dispersion of a simple width-modulated waveguide, where the structural unit contains only a single grating, as shown in Fig. 2(a). By introducing a double grating within this single structural unit, the BZ of the modulated waveguide is folded to half its original size. Interestingly, the waveguide mode originally located below the light cone is folded above it. Notably, the Γ point originates from the boundary of the BZ of the unfolded lattice after band folding and retains the high-quality (Q) factor inherited from the waveguide below the light cone, as shown in Figs. 2(b) and 2(c). Consequently, the waveguide near the Γ point exhibits extremely low radiative loss, even though its band lies above the light cone.

To validate this BZ-folded BICs mechanism, we introduce a relative shift parameter δ between the two modulated gratings. As δ deviates from zero, the BICs transition into a quasi-BICs state. Importantly, the Q factor decreases rapidly with increasing δ, as demonstrated in Fig. 2(d). This reduction in Q factor arises from the breakdown of destructive interference between the two radiation channels. Figure 2(e) compares the Q factor at $\delta = 0$ and $\delta = 0.02$ for the two bands at the Γ point, revealing that the Q factor of BICs is five orders of magnitude higher than that of quasi-BICs. Correspondingly, the BICs-assisted SSH-like waveguide exhibits significantly lower propagation loss compared to the quasi-BICs-assisted waveguide, as shown in Fig. 2(f).

In addition to reducing radiation loss induced by grating modulation on the waveguide, the topological interface formed by combining two types of 1D photonic crystal waveguides can introduce mode-mismatch-related loss, as illustrated in Figs. 3(a) and 3(b). This mode mismatch can be exemplified by the differing eigen-fields of type-A and type-B waveguides for the same band, as shown in Fig. 1(d). To mitigate this mode mismatch at the topological interface, we adiabatically decrease the modulation depth to zero as light propagates across the interface, as illustrated in Fig. 3(c). Through this optimization of the grating modulation profile, the mode-mismatch loss is significantly suppressed, achieving a reduction by two orders of magnitude compared to the unoptimized case, as demonstrated in Figs. 3(d)–3(f).

To theoretically calculate the photon-pair flux via SFWM, we select the pump frequency $\omega_p = 194.93\,\mathrm{THz}$, signal frequency $\omega_s = 195.05\,\mathrm{THz}$, and idler frequency $\omega_i = 194.81\,\mathrm{THz}$, satisfying the energy conservation condition $2\omega_p - \omega_s - \omega_i = 0$. The pump wave is positioned at the Γ point, resulting in a pump wavevector $\beta_p = 0$. Due to the high-symmetry dispersion of the superlattice waveguide, the wavevectors of the signal (β_s) and idler ((β_i) waves naturally satisfy $\beta_s + \beta_i \approx 0$. These conditions ensure that the momentum conservation relation for SFWM, $2\beta_p - \beta_s - \beta_i \approx 0$, is also satisfied. The large group refractive indices of the pump ($n_p = 12$), signal ($n_s = 21$), and idler ($n_i = 34$) waves, combined with the ultra-low propagation loss ($\alpha \approx 0.25\,\mathrm{dB/mm}$), enable a photon-pair generation rate in the BICs-assisted superlattice waveguide that is two orders of magnitude higher than that in conventional silicon-nanowire waveguides. After considering the additional side wall scattering loss ($\alpha \approx 0.04\,\mathrm{dB/mm}$) [36], we calculated the generation of the photon-pair flux. In contrast, the photon-pair generation rates in quasi-BICs-assisted and non-optimized BICs-assisted waveguides decay rapidly due to high propagation losses, as shown in Fig. 3(g).

Conclusion. In this work, we propose a scheme of optimized grating structures on a conventional silicon-nanowire waveguide. Benefiting from the BICs and the slow light effect, this modulated silicon-nanowire waveguide has achieved a two-order-of-magnitude enhancement in SFWM. Our proposed scheme is not limited to SFWM on the SOI platform. It can be extended to various nonlinear optical processes in other nonlinear optical materials. Although the concept is theoretical, it is fully implementable using mature SOI fabrication techniques. These results open new avenues for the development of highly integrated, ultra-low-loss, and versatile nonlinear nanophotonic devices.

Funding. National Key Research and Development Program of China (2023YFB2805700); National Natural Science Foundation of China (12174187, 62288101, 92163216, 92463308); Natural Science Foundation of Jiangsu Province, China (BK20240164, BK20243009); Fundamental Research Funds for the Central Universities, China (2024300329).

Disclosures. The authors declare no conflicts of interest.

Data availability. Data underlying the results presented in this paper are not publicly available at this time but may be obtained from the authors upon reasonable request.

Supplemental document. See Supplement 1 for supporting content.

REFERENCES

1. J. Wang, F. Sciarrino, A. Laing, *et al.*, Nat. Photonics **14**, 273 (2020).
2. W. Luo, L. Cao, Y. Z. Shi, *et al.*, Light-Sci. Appl. **12**, 175 (2023).
3. A.A. Politi, M. J. Cryan, J. G. Rarity, *et al.*, Science **320**, 646 (2008).
4. J. W. Silverstone, D. Bonneau, K. Ohira, *et al.*, Nat. Photonics **8**, 104 (2014).
5. H. Jin, F. M. Liu, P. Xu, *et al.*, Phys. Rev. Lett. **113**, 103601 (2014).
6. J. B. Spring, P. L. Mennea, B. J. Metcalf, *et al.*, Optica **4**, 90 (2017).
7. R.-J. Ren, Y.-H. Lu, Z.-K. Jiang, *et al.*, Photon. Res. **10**, 456 (2022).
8. A.A. Raymond, A. Zecchetto, J. Palomo, *et al.*, Phys. Rev. Lett. **133**, 233602 (2024).
9. H. Zeng, Z. Q. He, Y. R. Fan, *et al.*, Phys. Rev. Lett. **132**, 133603 (2024).
10. Y. Zheng, C. G. Zhai, D. J. Liu, *et al.*, Science **381**, 221 (2023).
11. J. E. Sharping, K. F. Lee, M. A. Foster, *et al.*, Opt. Express **14**, 12388 (2006).
12. S. Clemmen, K. P. Huy, W. Bogaerts, *et al.*, Opt. Express **17**, 16558 (2009).
13. M. Davanço, J. R. Ong, A. B. Shehata, *et al.*, Appl. Phys. Lett. **100**, 261104 (2012).
14. C. Xiong, C. Monat, A. S. Clark, *et al.*, Opt. Lett. **36**, 3413 (2011).
15. C. Monat, M. Ebnali-Heidari, C. Grillet, *et al.*, Opt. Express **18**, 22915 (2010).
16. S. Mittal, E. A. Goldschmidt, and M. Hafezi, Nature **561**, 502 (2018).
17. T. X. Dai, Y. T. Ao, J. M. Bao, *et al.*, Nat. Photonics **16**, 248 (2022).
18. C. C. Lu, Y. Z. Sun, C. Y. Wang, *et al.*, Nat. Commun. **13**, 2586 (2022).
19. F. J. Chen, H. R. Xue, Y. Pan, *et al.*, Phys. Rev. Lett. **132**, 156602 (2024).
20. S. Hughes, L. Ramunno, J. F. Young, *et al.*, Phys. Rev. Lett. **94**, 033903 (2005).
21. H. Friedrich and D. Wintgen, Phys. Rev. A **32**, 3231 (1985).
22. C. W. Hsu, B. Zhen, A. D. Stone, *et al.*, Nat. Rev. Mater. **1**, 16048 (2016).
23. M. Kang, T. Liu, C. T. Chan, *et al.*, Nat. Rev. Phys. **5**, 659 (2023).
24. M. Minkov, I. A. D. Williamson, M. Xiao, *et al.*, Phys. Rev. Lett. **121**, 263901 (2018).
25. H. N. Tang, C. DeVault, S. A. Camayd-Muñoz, *et al.*, Nano Lett. **21**, 914 (2021).
26. T. Dong, J. J. Liang, S. Camayd-Muñoz, *et al.*, Light-Sci. Appl. **10**, 10 (2021).
27. T. Dong, T. X. Dai, Y. Chen, *et al.*, Optica **11**, 799 (2024).
28. Z. Yu, X. Xi, J. Ma, *et al.*, Optica **6**, 1342 (2019).
29. C.-L. Zou, J.-M. Cui, F.-W. Sun, *et al.*, Laser Photonics Rev. **9**, 114 (2015).
30. F. Ye, Y. Qin, C. F. Cui, *et al.*, Photon. Res. **12**, 1322 (2024).
31. C. L. Li, J. H. He, M. Zhang, *et al.*, Laser Photonics Rev. **19**, e01998 (2025).
32. G. Y. Chen, Y. S. Liu, B. T. Ge, *et al.*, Laser Photonics Rev. **19**, e00380 (2025).
33. C. H. Han, Z. Zheng, H. W. Shu, *et al.*, Sci. Adv. **9**, eadi5339 (2023).
34. G. X. Chen, H. H. Wang, B. Chen, *et al.*, Nanophotonics **12**, 3603 (2023).
35. K. Guo, S. M. M. Friis, J. B. Christensen, *et al.*, Opt. Lett. **42**, 3670 (2017).
36. T. Horikawa, D. Shimura, and T. Mogami, MRS Commun. **6**, 9 (2016).